

of hydrogen from a methyl group, separated by a series of bonds in a cyclic array, which situated the transferring atom in close proximity to the initial radical center. A case in point is the isomerization of 2,4,6-tri-*tert*-butylphenyl radical.

The isomerization was observed over a very long temperature range ( $-26 \rightarrow -245$  °C). It was possible under these conditions to recognize unequivocally curvature of the Arrhenius plot, a large difference in the activation energies,  $[\Delta E_a]_D^H \gg 1.3$ , and a large, inverse ratio of the preexponential factors ( $A_H/A_D = 0.1 \rightarrow 0.01$ ) for H and D transfer. The experimentally determined  $k_H/k_D$  values rise from 80 at  $-30$  °C to 13 000 at  $-150$  °C, which is significantly larger than the maximum classical  $k_H/k_D = 260$  at  $-150$  °C.

### Concluding Remarks

The applications of the mechanistic criteria discussed above represent only a small sample of a growing number of cases. The large majority of these cases, thus far, involve cyclic processes of intramolecular H transfer, although in theory as well as known practice there is no evident restriction from application to intermolecular H transfer. The most visible accomplishments of this kinetic isotope effect approach to elucidating mechanistic features are the following: (1) the identification of tunneling and the factors which bring about the alteration in the dimensions of the reaction barrier;

(2) the direct characterization of transition-state geometry, i.e., linear or angular H transfer, and some first hand perception of the factors that control this previously neglected TS property; (3) the emergence of a "definite" criterion of concertedness in H-transfer processes, wherein the magnitudes of  $[\Delta E_a]_D^H$  and  $A_H/A_D$  are invoked in a quantitative way; (4) the basis for a call to reevaluate many earlier mechanistic conclusions derived from a single temperature measurement of  $k_H/k_D$  and an "eyeball" interpretation of such results. Values of  $A_H/A_D$  of extraordinary magnitude tend to vitiate this common practice among organic chemists interpreting isotope effects. Moreover, until suitable procedures of model calculations can be developed to account rigorously for temperature-independent isotope effects of extraordinary magnitude, previously calculated single temperature  $k_H/k_D$  values must be viewed with some suspicion. Whether an isotope effect is large, small, or intermediate (which is the language commonly used in such discussions) is devoid of significance until its temperature dependence is also known.

*I take this opportunity to acknowledge with gratitude the support of the Petroleum Research Fund, administered by the American Chemical Society, for some of these research studies as well as the contributions of all those whose names appear in the cited publications from these laboratories. Part of this work was also supported by a grant from the National Science Foundation (Grant 7911110).*

## Novel Radical Anions and Hydrogen Atom Tunneling in the Solid State

FFRANCON WILLIAMS\*

*Department of Chemistry, University of Tennessee, Knoxville, Tennessee 37996-1600*

ESTEL D. SPRAGUE\*

*Department of Chemistry, University of Cincinnati, Cincinnati, Ohio 45221*

*Received August 10, 1981 (Revised Manuscript Received August 9, 1982)*

While it has long been recognized that the exposure of solids to  $\gamma$  or X radiation at low temperatures results in the production of trapped radicals, it is perhaps less well-known that this technique has enabled the discovery of several novel and unusual paramagnetic

species. In this Account we are concerned largely with the characterization and chemical significance of the radical anions and radical-anion pairs formed from acetonitrile, methyl halides, and dimethyl sulfoxide.

Initially, these studies were severely complicated by the occurrence of hydrogen atom abstraction reactions by methyl radicals at low temperatures. Far from having only nuisance value, however, these reactions proved to be of intrinsic interest and provided an ideal proving ground for the demonstration of quantum tunneling.

### Experimental Aspects

Because  $\gamma$  or X-ray photons have high energies (1.17 and 1.33 MeV from  $^{60}\text{Co}$ ), it is a common misconception that molecules in an absorber are subjected to an extremely energetic process devoid of chemical specificity.

Ffrancon Williams, born in 1928 in North Wales, received his B.Sc. from University College, London, and an external Ph.D. from the University of London. After 10 years at the U.K. Atomic Energy Research Establishment at Harwell and 2 years as a research associate at Northwestern University, he joined the faculty of the University of Tennessee in 1961, where he is now an Alumni Distinguished Service Professor. He has been an NSF Visiting Scientist to Kyoto University (1965-1966) and a Guggenheim Fellow (1972-1973).

Estel D. Sprague was born in Kansas in 1944. He obtained his Ph.D. at the University of Tennessee and carried out postdoctoral research at the Institut für Strahlenchemie im Max-Planck-Institut für Kohlenforschung, Mülheim (Ruhr), and at the University of Wisconsin. He joined the University of Cincinnati faculty in 1974 and he is now Associate Professor of Chemistry.

In fact, the encounters of the  $\gamma$  rays themselves with the medium are *not* the typical events by which absorber molecules are energized. Actually, a single event in the  $\gamma$ -ray attenuation processes of photoelectric absorption and Compton scattering releases a high-energy (up to 600 keV for  $^{60}\text{Co}$   $\gamma$  rays) electron of limited range, which brings about the secondary ionization of a very large number of molecules in the medium,<sup>1</sup> thereby releasing additional electrons with low energies. It is not surprising, therefore, that high-energy irradiation provides a very suitable general method for the generation of radical ions by ionization and electron attachment.<sup>2</sup>

ESR spectroscopy is clearly the method of choice for the identification of radicals since the technique provides characteristic hyperfine patterns for each type of radical with high sensitivity. Although the correct analysis and assignment of an ESR spectrum allow radical identification from first principles, this can only be achieved with complete confidence if the spectrum is sufficiently well resolved. In particular, considerable care is needed in the analysis of anisotropically broadened spectra from randomly oriented solids. Undoubtedly the ideal way to identify and characterize a radical is to carry out a single-crystal study. In this way the analysis of the hyperfine structure can be verified at many orientations, and the determination of the hyperfine tensors yields complete information about the spin distribution.

If a single crystal cannot be prepared, we have found that the ESR examination of partially ordered samples<sup>3</sup> can be extremely helpful. Even for comparatively low degrees of order, the spectrum frequently shows a striking angular dependence such that, at optimum orientations in the magnetic field, enhanced intensities and greatly improved line resolution are achieved at the turning points or singularities in the powder pattern. For example, it has been shown that after the parallel features of a radical possessing axially symmetric tensors have been brought into prominence at one orientation, the perpendicular set can be intensified by rotation of the sample tube by 90°. In some cases it is possible to achieve almost complete discrimination such that only one set of features appears in the spectrum at the optimum orientation. This is a very useful aid in the analysis of powder spectra, since the spectrum of a randomly oriented sample may be unanalyzable owing to strong overlap between different features.

### Radical Anions of Acetonitrile

Acetonitrile has a solid-phase transition temperature of 216.9 K, just below the fusion temperature of 229.3 K.<sup>4</sup> The high-temperature phase is referred to as crystal I, the low-temperature phase as crystal II. Samples of either phase may be studied at much lower

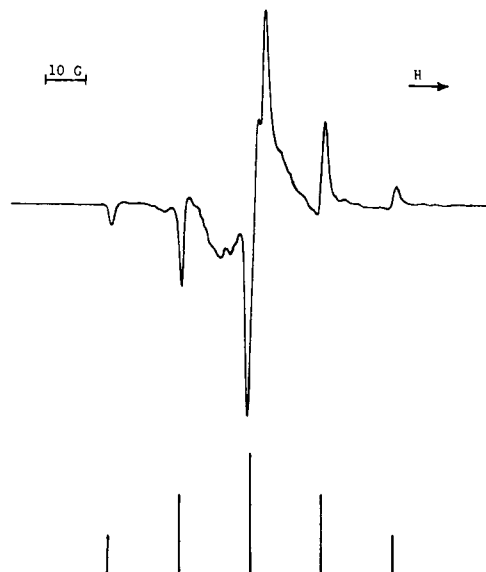


**Figure 1.** First-derivative ESR spectrum of a polycrystalline sample of  $\gamma$ -irradiated crystal I of  $\text{CD}_3\text{CN}$  at 77 K recorded at low microwave power (0.008 mW).

temperatures, however, since crystal I is invariably obtained unless the sample is cooled slowly through the transition temperature.

It was first observed<sup>5</sup> about 18 years ago that crystal I of acetonitrile becomes purple upon  $\gamma$  irradiation at 77 K. Although the color center was initially hypothesized<sup>5</sup> to be triplet-state acetonitrile, this was soon rejected<sup>6</sup> in favor of an assignment to trapped electrons on the basis of its photobleaching characteristics. An ESR spectrum, however, was not observed until very low microwave power levels were employed.<sup>7</sup> Of primary interest was the observation of well-resolved hyperfine structure in the ESR spectrum showing interaction of the unpaired electron with *two* acetonitrile molecules.<sup>7,8</sup> While some properties of this dimeric center, particularly the photobleaching and facile power saturation of its ESR signal, were found to closely resemble those of physically trapped electrons, the well-defined anisotropic hyperfine structure<sup>7b</sup> was in marked contrast to the structureless singlet characteristic of trapped electrons in glassy matrices.<sup>9</sup>

These significant ESR results from our laboratory<sup>7,8</sup> were soon confirmed by another group,<sup>10</sup> who preferred, however, to describe this dimeric center as a radical anion weakly bonded to a neighboring molecule rather than as a trapped electron bound to two acetonitrile molecules.<sup>7,11</sup> This suggestion<sup>10</sup> turned out to be correct, but a clear distinction<sup>12</sup> between the two descrip-

(5) Dunbar, D.; Hale, D.; Harrah, L.; Rondeau, R.; Zacanycz, S. "Developments in Applied Spectroscopy"; Forrette, J. E., Lanterman, E., Eds.; Plenum: New York, 1964; Vol. 3, p 361.

(6) Ayscough, P. B.; Collins, R. G.; Kemp, T. J. *J. Phys. Chem.* 1966, 70, 2220.

(7) (a) Bonin, M. A.; Tsuji, K.; Williams, F. *Nature (London)* 1968, 218, 946. (b) Bonin, M. A.; Takeda, K.; Williams, F. *J. Chem. Phys.* 1969, 50, 5423.

(8) Bonin, M. A. Ph.D. Thesis: The University of Tennessee, 1969.

(9) Tsuji, K.; Williams, F. *Trans. Faraday Soc.* 1968, 65, 1718.

(10) Eglund, R. J.; Symons, M. C. R. *J. Chem. Soc. A* 1970, 1326.

(11) The possibility that the electron is trapped specifically in the dipole fields of acetonitrile and other polar molecules was also considered: Bonin, M. A.; Takeda, K.; Tsuji, K.; Williams, F. *Chem. Phys. Lett.* 1968, 2, 363. This concept, however, seems to be more applicable to the negative ion states of polar molecules in the gas phase; for a review of the latter subject, see: Jordan, K. D. *Acc. Chem. Res.* 1979, 12, 36.

(1) Friedlander, G.; Kennedy, J. W.; Miller, J. M. "Nuclear and Radiochemistry", 2nd ed.; Wiley: New York, 1964; p 108.

(2) For a comprehensive discussion of radiation effects, see: "Fundamental Processes in Radiation Chemistry"; Ausloos, P., Ed.; Wiley: New York, 1968.

(3) Kasai, P. H.; Weltner, Jr., W.; Whipple, E. B. *J. Chem. Phys.* 1965, 42, 1120. Fierz, H.; Von Zelewsky, A. *Inorg. Chem.* 1971, 10, 1556. Davis, P. H.; Belford, R. L. *Ibid.* 1971, 10, 1557. For a textbook illustration of this partial orientation effect and additional references, see: McNeill, R. I.; Williams, F.; Yim, M. B. *Chem. Phys. Lett.* 1979, 61, 293.

(4) Putnam, W. E.; McEachern, D. M.; Kilpatrick, J. E. *J. Chem. Phys.* 1965, 42, 749.

Table I  
 ESR Parameters and Spin Densities for Radical Anions of Acetonitrile<sup>a</sup>

radical anion	$g_1$	$g_2$	$g_3$	nucleus	$A_1/G$	$A_2/G$	$A_3/G$	$\rho_s^b$	$\rho_p^b$
$(\text{MeCN})_2^-$	2.0024	2.0046 <sup>c</sup>	2.0007	<sup>14</sup> N	17.5	0 ± 3	0 ± 3	0.01	0.34
				<sup>13</sup> C(CN)	5	8	0	<0.01	0.13
				<sup>13</sup> C(Me) <sup>d</sup>	22.8	18.7	17.4	0.02	0.05
MeCN <sup>-</sup>	2.0022	2.0031	1.9991	<sup>14</sup> N <sup>d</sup>	12.8	8.2	3.2	0.01	0.55
				<sup>13</sup> C(CN)	71.7	59.6	53.0	0.054	0.19
				<sup>13</sup> C(Me)	$A_{\text{iso}} \sim 88 \text{ G}$			0.08	

<sup>a</sup> Reference 16. The uncertainties in the  $g$  values are approximately  $\pm 0.0004$ , while those in the hyperfine values are about  $\pm 0.5 \text{ G}$ . <sup>b</sup> The spin densities for  $(\text{MeCN})_2^-$  should all be multiplied by two to obtain the sum over the dimer. <sup>c</sup> This value is probably too high. See ref 14. <sup>d</sup> The principal axes for this tensor are not coincident with the others in this radical.

tions became possible only as the result of a thorough ESR study,<sup>13-16</sup> the main features of which are now described.

When crystal I of acetonitrile,  $\text{CH}_3\text{CN}$ , or any of its isotopic variations is exposed to  $\gamma$  radiation in the dark at 77 K, the main species observed by ESR and optical spectroscopy are  $\text{CH}_2\text{CN}$  and the dimer radical anion,  $(\text{CH}_3\text{CN})_2^-$ , or the corresponding isotopic species. The ESR spectrum of  $(\text{CH}_3\text{CN})_2^-$  in  $\text{CH}_3\text{CN}$  is obscured, however, by proton hyperfine broadening and the overlapping  $\text{CH}_2\text{CN}$  spectrum,<sup>14</sup> although it can be observed, complete with resolved proton hyperfine structure, for certain orientations of single crystals of  $\text{CH}_3\text{CN}$ .<sup>15</sup> Most measurements, therefore, have been made on deuterated material.

A typical spectrum for irradiated, polycrystalline  $\text{CD}_3\text{CN}$  is shown in Figure 1, where it is evident that the background signals, primarily from  $\text{CD}_2\text{CN}$ , are confined to a reasonably narrow region in the center of the spectrum. The prominent set of quintet features is due to  $(\text{CD}_3\text{CN})_2^-$  and corresponds to the parallel components of the spectrum arising from the interaction of the unpaired electron with two equivalent <sup>14</sup>N ( $I = 1$ ) nuclei, the hyperfine tensors having nearly cylindrical symmetry. The apparent absence of perpendicular features results from the near zero value for the perpendicular elements of the <sup>14</sup>N hyperfine tensors.

For complete characterization of this species, single crystals of various isotopically labeled molecules were grown in 1-mm i.d. tubes by slow freezing just below the melting point, followed by quenching to 77 K and exposure to  $\gamma$  radiation. Representative spectra are shown in Figure 2a for  $(^{12}\text{CD}_3^{12}\text{C}^{14}\text{N})_2^-$  and  $(^{12}\text{CD}_3^{13}\text{C}^{14}\text{N})_2^-$ . Hyperfine interaction with pairs of magnetically equivalent nuclei derived from two acetonitrile molecules was observed<sup>16</sup> for all the labeled species examined, including those from  $^{12}\text{CD}_3^{12}\text{C}^{14}\text{N}$ ,  $^{12}\text{CD}_3^{12}\text{C}^{15}\text{N}$ ,  $^{12}\text{CD}_3^{13}\text{C}^{14}\text{N}$ , and  $^{13}\text{CD}_3^{12}\text{C}^{14}\text{N}$ . It follows necessarily that two acetonitrile molecules are required to form this

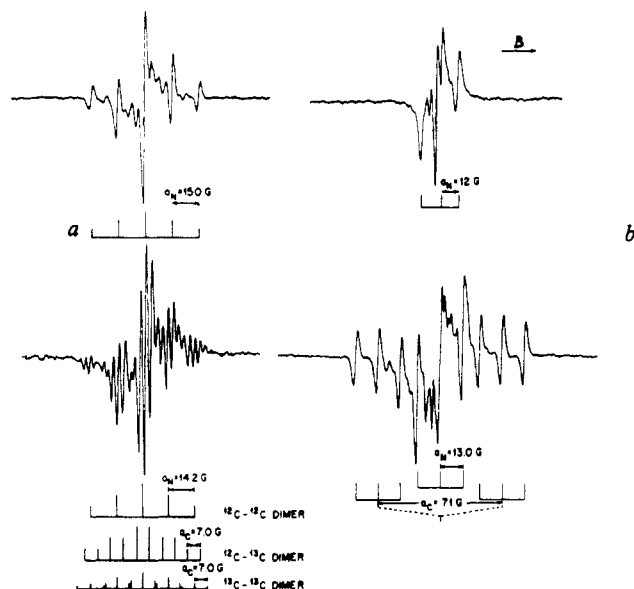


Figure 2. First-derivative ESR spectra of (a) the dimer radical anion of acetonitrile (crystal I) and (b) the monomer radical anion of acetonitrile (crystal II) in  $\gamma$ -irradiated single crystals of  $^{12}\text{CD}_3^{12}\text{C}^{14}\text{N}$  (upper spectra) and  $^{12}\text{CD}_3^{13}\text{C}^{14}\text{N}$ , enriched with 55% <sup>13</sup>C, (lower spectra) at 77 K.

species and, furthermore, that it possesses a center of symmetry. From the orientation dependence of the hyperfine splittings, hyperfine tensors were determined,<sup>16</sup> and from these tensors experimental spin densities were derived in the usual manner.<sup>17</sup>

These results (Table I) show that most of the spin density (0.68) is concentrated in the nitrogen 2p orbitals, with much lesser amounts in the 2p orbitals of the cyanide and methyl carbons. Since only very small spin densities ( $<0.01$ ) reside in the 2s orbitals of the cyanide carbons, this indicates that the acetonitrile molecules retain their linearity in the dimer anion. Another significant feature is that the sum of the spin densities over all the atoms in the two acetonitrile molecules comprising this species is approximately unity. This constitutes conclusive evidence that the unpaired electron resides entirely within the orbitals of the two molecules. The purple color center is therefore more appropriately labeled as a dimer radical anion rather than a trapped electron.

Any antiparallel configuration of two acetonitrile molecules fulfills the requirement that the dimer radical anion be centrosymmetric. Four possible arrangements, 1a-1d, are shown below. Of course, a continuous range of possible geometries exists between those shown. For

(12) This distinction is based on a cavity model for trapped electrons that largely excludes them from the orbitals of the matrix molecules. For a detailed discussion of trapped electrons in glasses, see: Kevan, L. *Adv. Radiation Chem.* 1974, 4, 181; *Acc. Chem. Res.* 1981, 14, 138. In contrast, ESR studies of excess-electron species in liquids do not differentiate clearly between a solvated cavity model and that of a solvated radical anion complex. Both of these descriptions have been invoked to explain the properties of solvated electrons in polar fluids: Golden, S.; Tuttle, T. R. *J. Phys. Chem.* 1978, 82, 944. Symons, M. C. R. *Radiat. Phys. Chem.* 1981, 17, 425.

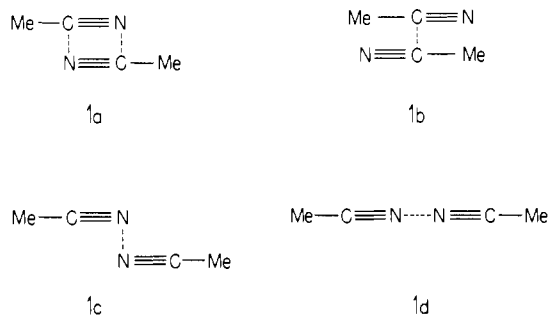
(13) Sprague, E. D.; Takeda, K.; Williams, F. *Chem. Phys. Lett.* 1971, 10, 299.

(14) Sprague, E. D.; Ph.D. Thesis: The University of Tennessee, 1971.

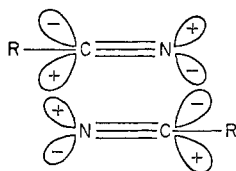
(15) Gillbro, T.; Takeda, K.; Williams, F. *J. Chem. Soc., Faraday Trans. 2* 1974, 70, 465.

(16) (a) Bonin, M. A.; Chung, Y. J.; Sprague, E. D.; Takeda, K.; Wang, J. T.; Williams, F. *Nobel Symp.* 1972, 22, 103. (b) Takeda, K.; Ph.D. Thesis, Kyoto University, 1971.

(17) Atkins, P. W.; Symons, M. C. R. "The Structure of Inorganic Radicals"; Elsevier: Amsterdam, 1967; p 20.



each of these arrangements, INDO calculations<sup>18</sup> correctly predict the presence of large spin densities in the in-plane p orbitals of the cyanide groups as the molecules are allowed to approach each other along the interatomic axes shown, but only structure **1b** could reproduce the large experimental ratio of the spin density in the nitrogen 2p orbitals to that in the cyanide carbon 2p orbitals. In our opinion, however, this latter observation is less significant than the fact that dimer radical anions having virtually the same <sup>14</sup>N hyperfine structure as that described for acetonitrile are also produced in crystalline phases of propionitrile,<sup>14</sup> succinonitrile,<sup>7b</sup> and adiponitrile.<sup>16</sup> This result argues against structure **1b** since the placement of these larger molecules to achieve a similar configuration would appear to be sterically unfavorable. In fact, this experimental work pointing to an almost identical dimer structure for each of three different nitriles is suggestive of a strong interaction between like cyanide groups as in the heterocyclic structure **1a**.<sup>19</sup> Moreover, as shown below,



the  $B_u$  SOMO of this intuitively more appealing ( $C_{2h}$ ) structure is bonding between the molecules, and this would explain why the spin distribution is biased in favor of the more electronegative nitrogen atoms.

The purple color of the dimer radical anion is due to an optical absorption band (Figure 3) which begins at about 875 nm in the near-IR region and extends completely through the visible region, with a maximum at 510 nm.<sup>20</sup> In terms of structure **1a**, this band can readily be assigned to the allowed  $B_u \rightarrow A_g$  "charge-resonance" transition in which the unpaired electron is promoted from the bonding to the antibonding combination of in-plane  $\pi^*$  orbitals. Analogous charge-resonance transitions for olefin and aromatic dimer radical cations<sup>21</sup> and for the 2,2'-paracyclophane radical anion<sup>22</sup> are also characterized by strong broad absorp-

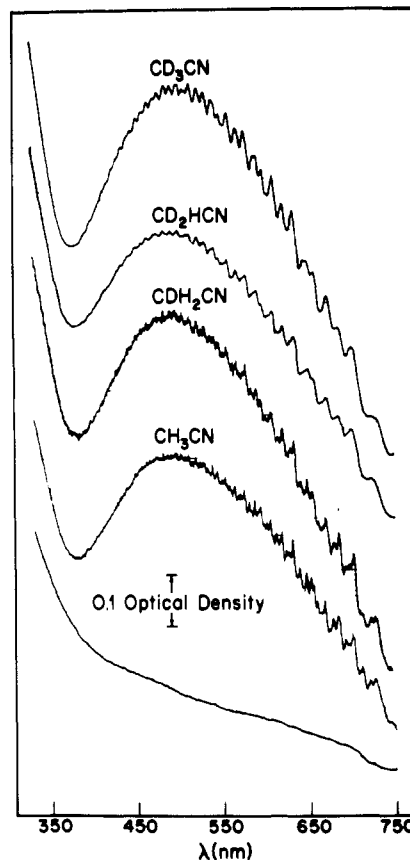


Figure 3. Visible absorption spectra of  $\gamma$ -irradiated crystal I of  $CD_3CN$ ,  $CD_2HCN$ ,  $CDH_2CN$ , and  $CH_3CN$  at 77 K. The lowest trace is the blank spectrum of the  $CD_3CN$  sample after in situ photobleaching.

tions in the visible or near-IR regions. Thus, the presence of a similar band in the  $\gamma$ -irradiated acetonitrile crystal I nicely corroborates the ESR evidence for dimer radical anion formation.

It is also noteworthy that this charge-resonance band for  $(MeCN)_2^-$  displays considerable vibrational fine structure, which as expected differs in detail in the series  $CH_3CN$ ,  $CH_2DCN$ ,  $CHD_2CN$ ,  $CD_3CN$ ,<sup>14,23</sup> as shown in Figure 3. A second absorption band, with a maximum in the UV region at about 305 nm, can also be assigned to the dimer radical anion.<sup>14,23</sup> All of the optical spectra were determined at 77 K from polycrystalline samples by using 1-mm pathlength cells and compensating for scattering by means of neutral density filters.

Definitive evidence that the species responsible for the purple color and the dimer ESR spectrum is an anion rather than a cation comes from experiments in which methyl halides were used as electron scavengers.<sup>24</sup> In mixtures containing 10 mol %  $CH_3Cl$  or  $CH_3Br$  in  $CD_3CN$ , dissociative electron capture by the methyl halides was observed by ESR (vide infra), and the formation of the optical band and ESR absorption associated with the dimer radical was prevented. Thus the dimer species must result from electron attachment to acetonitrile.

(18) Kerr, C. M. L., unpublished results.

(19) The heterocyclic ring dimer  $(MeCN)_2^-$  represented by structure **1a** possesses 21 valence electrons in the ring system. The SOMO is therefore quite analogous to the HOMO of the 22 valence electron dimer  $(NO)_2$ , which is formed with a centrosymmetric ( $C_{2h}$ ) structure in the crystalline state. See: Cotton, F. A.; Wilkinson, G. "Advanced Inorganic Chemistry", 3rd ed.; Wiley: New York, 1972; p 354.

(20) Holloman, H. L.; Sprague, E. D.; Williams, F. *J. Am. Chem. Soc.* 1970, 92, 429.

(21) Badger, B.; Brocklehurst, B. *Trans. Faraday Soc.* 1969, 65, 2576, 2582, 2588; 1970, 66, 2939.

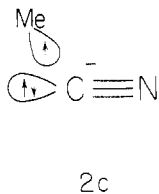
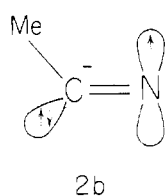
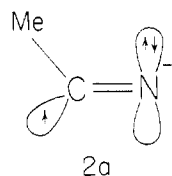
(22) Ishitani, A.; Nagakura, S. *Mol. Phys.* 1967, 12, 1. Dimer radical anions of several olefin derivatives have also been detected in pulse radiolysis studies: Arai, S.; Kira, A.; Imamura, M. *J. Phys. Chem.* 1977, 81, 110.

(23) Holloman, H. L.; M.S. Thesis: The University of Tennessee, 1970.

(24) Sprague, E. D.; Williams, F. *J. Chem. Phys.* 1971, 54, 5425.

A peculiarity of this system, which is perhaps typical of the unpredictability of the results in irradiated solids, is that  $\gamma$  irradiation of crystal II of acetonitrile at 77 K does not result in the formation of the purple dimer radical anion. What is actually produced is the red-brown monomer radical anion,  $\text{MeCN}^-$ . This identification<sup>25</sup> is based largely on ESR studies of  $^{12}\text{CD}_3^{12}\text{C}^{14}\text{N}$  and  $^{12}\text{CD}_3^{13}\text{C}^{14}\text{N}$ . In each case the ESR spectrum showed that the unpaired electron interacts with the nuclei in only one molecule. Although it proved to be extremely difficult to grow single crystals of this phase, this objective was achieved in some instances, as illustrated by the well-resolved spectra from  $^{12}\text{CD}_3^{12}\text{C}^{14}\text{N}$  and  $^{12}\text{CD}_3^{13}\text{C}^{14}\text{N}$  in Figure 2b, so that hyperfine tensors could be determined.<sup>16</sup> These are presented in Table I, along with the experimental spin densities derived from them. The spin densities in the p orbitals on the methyl carbon atom were not determined, but since it is reasonable to assume  $\text{sp}^3$  hybridization, the total spin density on the atom is 0.31, and the sum of the spin densities over all the atoms in this species is close to unity.

The structure of  $\text{MeCN}^-$  is brought out most clearly by the large principal values of the cyanide  $^{13}\text{C}$  hyperfine tensor,<sup>16</sup> which are comparable to the values obtained for the  $^{13}\text{C}$  tensor in the isostructural molecule  $\text{HCN}^-$ .<sup>26</sup> Furthermore, the C-C-N angle calculated by Coulson's formula<sup>27</sup> from the p/s hybridization ratio of spin densities on the cyanide carbon (3.5) is  $130^\circ$ , in excellent agreement with the value of  $131^\circ$  determined for  $\text{HCN}^-$ .<sup>26</sup> These anions are structurally similar to their neutral isoelectronic counterparts  $\text{CH}_3\text{CO}$  and  $\text{HCO}$ , with the unpaired electron occupying a  $\sigma$  orbital with appreciable spin density in an  $\text{sp}^n$  hybrid on the cyanide carbon, as illustrated by the valence-bond formula 2a. However, the presence of comparable spin



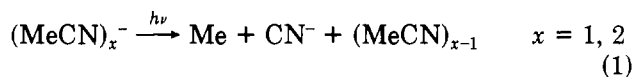
densities on the methyl carbon and the nitrogen suggests that the representations 2b and 2c also contribute to the electronic structure of the radical since these conform to the  $\sigma$  symmetry of the molecular orbital.

The contrast between the bent geometry of  $\text{MeCN}^-$  and the near linearity of the acetonitrile molecules in  $(\text{MeCN})_2^-$  is a reflection of the way in which these molecules can accommodate the extra electron by lowering the energy of the SOMO. Whereas this can only

occur by bending in the monomer species as predicted by Walsh's rules,<sup>28</sup> stabilization of the dimer anion is provided by the overlap of the in-plane  $\pi^*$  orbitals so that bending should be much less important in this case, as observed.

The optical spectrum of the monomer radical anion consists of a broad structureless band with a maximum at 430 nm, identical spectra being obtained in the series  $\text{CH}_3\text{CN}$ ,  $\text{CH}_2\text{DCN}$ ,  $\text{CHD}_2\text{CN}$ ,  $\text{CD}_3\text{CN}$ .<sup>14,23</sup> Despite the difference in molecular geometry referred to above, it is tempting to assign this band to the same transition responsible for the short (305 nm) wavelength band of the dimer radical anion, the red shift for the monomer paralleling the findings for other pairs of radical ions.<sup>21,22</sup> Since the "charge-resonance" band is unique to the dimer species, a second band at longer wavelengths is neither expected nor observed for the monomer radical anion.

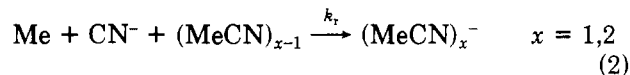
Both the monomer and dimer radical anions are readily photobleached,<sup>6,7,13,25</sup> the optical and ESR spectra being removed on exposure to red ( $\lambda > 640$  nm) or white light, and the only product observable by ESR is the methyl radical. This has been verified for all the isotopically labeled species studied, so that the overall processes can be represented as in eq 1.



Evidently, the methyl radicals produced by photobleaching the radical anions in single-crystal samples are themselves oriented. This is shown by the orientation dependence of the ESR spectrum of  $^{13}\text{CD}_3$  radicals, which verifies that they are not tumbling randomly, but rather are spinning or precessing about the axis of the p orbital containing the unpaired electron.<sup>16</sup> In single crystals of crystal II of  $^{12}\text{CD}_3^{13}\text{C}^{14}\text{N}$ , a very slight  $^{13}\text{C}$  hyperfine splitting is observed for the methyl radicals. It is readily interpreted<sup>29</sup> as an extremely weak  $\sigma$  interaction between the unpaired electron in the p orbital of the methyl radical and the lone pair of electrons in the sp hybrid orbital of the cyanide ion.

### Methyl Radical Reactions at Low Temperatures

The methyl radicals produced in acetonitrile by reaction 1 presented a most intriguing puzzle. It was discovered that  $\text{CD}_3$  radicals in  $\text{CD}_3\text{CN}$  reverted completely to radical anions on standing in the dark whereas under the same conditions at 77 K the  $\text{CH}_3$  radicals simply disappeared in  $\text{CH}_3\text{CN}$  without regenerating radical anions.<sup>7a,25</sup> This remarkable "all-or-nothing" isotope effect is now easily understood in terms of a simple kinetic competition between two parallel first-order processes.<sup>30</sup> The reaction mechanism is as shown in eq 2 and 3. Reaction 2 is just the



thermal reverse of reaction 1, and reaction 3 is the ab-

(25) Takeda, K.; Williams, F. *Mol. Phys.* 1969, 17, 677.

(26) Adrian, F. J.; Cochran, E. L.; Bowers, V. A.; Weatherly, B. C. *Phys. Rev.* 1969, 177, 129.

(27) Coulson, C. A. "The Shape and Structure of Molecules"; Clarendon: Oxford, 1973; p 43.

(28) Walsh, A. D. *J. Chem. Soc.* 1953, 2288.

(29) Sprague, E. D.; Takeda, K.; Wang, J. T.; Williams, F. *Can. J. Chem.* 1974, 52, 2840.

(30) Takeda, K.; Williams, F. *J. Phys. Chem.* 1970, 74, 4007.

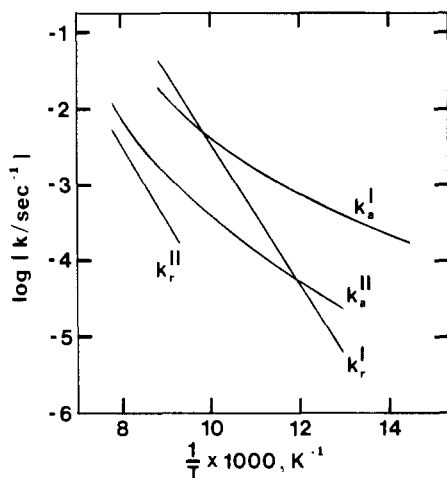


**Figure 4.** Arrhenius plot of the first-order rate constants for methyl radical reactions in  $\gamma$ -irradiated and photobleached crystal I and II of acetonitrile.  $k_a$  refers to hydrogen atom abstraction, and  $k_r$  refers to the thermal recovery reaction in  $\text{CH}_3\text{CN}$ .

straction of a hydrogen atom from an adjacent molecule in the crystalline matrix.

Both optical and ESR methods have been used to study these reactions. In all experiments the optical and ESR spectra of the radical anions were found to be completely correlated, showing conclusively that both spectra belong to the same species. The strikingly different results for  $\text{CH}_3\text{CN}$  and  $\text{CD}_3\text{CN}$  are simply a reflection of quantitative details in this mechanism. First, reaction 3 is characterized by such a large primary H/D isotope effect that it is effectively completely suppressed in  $\text{CD}_3\text{CN}$ . Thus, only the recovery reaction is observed. Second, the abstraction reaction in  $\text{CH}_3\text{CN}$  is so much faster than the recovery reaction at the experimentally convenient temperature of 77 K that only the abstraction reaction is observed.

It is logical to assume that the recovery reaction occurs because the products of the photobleaching reaction are constrained by the matrix to remain adjacent to each other.<sup>31-33</sup> Its rate has been measured at a number of temperatures in both crystalline phases of  $\text{CD}_3\text{CN}$ ,<sup>7a,16,23,30,34,35</sup> Within experimental error, the activation energy is the same in both phases,  $4.8 \pm 0.6$  kcal/mol. The actual first-order rate constants, however, are approximately 2 orders of magnitude smaller for the recovery of the monomer radical anion in crystal II than for the recovery of the dimer radical anion in crystal I.

The recovery reaction is only observed in  $\text{CH}_3\text{CN}$  at temperatures above 77 K.<sup>30</sup> Since the activation energy of reaction 2 is larger than that of reaction 3 (vide infra), it becomes more and more competitive at higher temperatures, as is evident in Figure 4. By determining both the apparent rate constant for methyl radical

decay and the fraction undergoing the recovery reaction, both rate constants may be calculated.<sup>35</sup> It was found that the recovery reaction in both phases of  $\text{CH}_3\text{CN}$  is characterized by the same activation energy as in both phases of  $\text{CD}_3\text{CN}$ .<sup>16,34</sup> At any particular temperature in either phase, the rate constant of the recovery reaction for  $\text{CD}_3$  radicals is some 3 or 4 times larger than that for  $\text{CH}_3$  radicals.<sup>16,34</sup> This inverse deuterium isotope effect is a property of the methyl radical reactants and is not attributable to the deuteration of the matrix since a similar result is found for the  $\text{CH}_3$  and  $\text{CD}_3$  radicals produced together in a mixed matrix of crystal I consisting predominantly of  $\text{CD}_3\text{CN}$ .<sup>16,31</sup>

The similar isotope effects and activation energies for the recovery of the monomer and dimer radical anions strongly suggest a common transition state for both of these reactions. This is intuitively reasonable if it is supposed that the recovery of the dimer radical anion in crystal I involves the formation of the monomer radical anion as an intermediate, rate-determining step. The difference in rate constants for the recovery of the two radical anions at a particular temperature may be attributed to differences in the steric disposition of the reaction partners in the two crystalline forms.

The observation of hydrogen atom abstraction at low temperature is highly significant. Definitive evidence for this reaction was first obtained in crystal I of acetonitrile through simultaneous monitoring by ESR of the decay of the  $\text{CH}_3$  radicals and the growth of the  $\text{CH}_2\text{CN}$  radicals.<sup>35</sup> The two independent values for the abstraction rate constant determined in this way agreed within experimental error, both at 77 K and at 87 K. Optical measurements were also carried out at 87 K on the series  $\text{CH}_3\text{CN}$ ,  $\text{CH}_2\text{DCN}$ ,  $\text{CHD}_2\text{CN}$ ,  $\text{CD}_3\text{CN}$ , and the abstraction rate constant was found to vary linearly with the number of H atoms in the acetonitrile molecule.<sup>35</sup> This provides clear verification that reaction 3 is a simple H atom abstraction process with a very large primary H/D isotope effect.

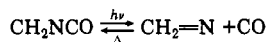
Additional studies have extended observation of the abstraction reaction both to crystal II of acetonitrile and to a wider temperature range,<sup>34,36</sup> as shown in Figure 4. Two salient features emerge. First, the abstraction reaction is a factor of 10 to 15 times slower in crystal II than in crystal I. Second, Arrhenius plots of the abstraction rate constants are not linear. In crystal I, for example, the apparent activation energy increases from about 0.8 kcal/mol at 69 K to 3.2 kcal/mol at 113 K.<sup>36</sup> In the gas phase, on the other hand, a value of  $10.0 \pm 0.5$  kcal/mol was obtained over the temperature range from 373 to 573 K.<sup>37</sup>

An attractive explanation for the ready occurrence of hydrogen atom abstraction at low temperatures, including the large isotope effects and nonlinear Arrhenius plots, is provided by the hypothesis of large quantum mechanical tunneling corrections to the reaction rate. Exact, one-dimensional tunneling calculations provide, in fact, a quantitative explanation of the observed effects, showing that both the gas-phase and the solid-phase results may be understood in terms of a single Gaussian-shaped potential energy barrier.<sup>38</sup>

(31) Sprague, E. D. *J. Phys. Chem.* 1977, 81, 516.

(32) Independent evidence is provided in ref 31 that translational diffusion of radicals in acetonitrile at 77 K does not occur.

(33) A similar photobleaching-recovery cycle is observed for the  $\text{CH}_2\text{NCO}$  radical



in irradiated methyl isocyanate. Fujiwara, M.; Tamura, N.; Hirai, H. *Bull. Chem. Soc. Jpn.* 1973, 46, 701.

(34) Takahashi, K. M.S. Thesis: The University of Tennessee, 1972. Skelton, J. D.; Takahashi, K.; Williams, F., unpublished results.

(35) Sprague, E. D.; Williams, F. *J. Am. Chem. Soc.* 1971, 93, 787.

(36) Wang, J. T. Ph.D. Thesis: The University of Tennessee, 1972.

(37) Wijnen, M. H. *J. Chem. Phys.* 1954, 22, 1074.

(38) Le Roy, R. J.; Sprague, E. D.; Williams, F. *J. Phys. Chem.* 1972, 76, 546.

An alternative to the tunneling explanation is the hypothesis of drastic modification of the potential energy surface for the reaction upon going to the solid state. Such effects would be difficult to predict, but an experimental test is possible, since only the tunneling hypothesis would explain a dramatic enhancement of the primary isotope effect above the nontunneling maximum expected on the basis of zero-point energy differences.<sup>38,39</sup> For acetonitrile this maximum is 1500 at 77 K.<sup>31</sup> Therefore rather difficult, long-term measurements of an extremely slow reaction are required. Such measurements were carried out over a period of several months at 77 K for samples of crystal I of acetonitrile containing both CD<sub>3</sub>CN and CH<sub>3</sub>CN.<sup>31</sup> A detailed analysis of the behavior observed in these samples showed that the isotope effect is at least 28 000, well beyond the 1500 limit. Thus the tunneling hypothesis is very strongly supported.

The tunneling corrections to the abstraction rate at low temperature are so large that the classical reaction rate would be negligible.<sup>38</sup> The rate is therefore likely to be very sensitive to even slight changes in the barrier width and height.<sup>36,38</sup> It is consequently not surprising that the rates in the two crystalline forms differ significantly. In fact, simply replacing the CN<sup>-</sup>, which is necessarily adjacent to the methyl radical produced in the solid by means of reaction 1, with Br<sup>-</sup> results in a significant perturbation. Thus the abstraction rate constant in crystal I was found to be reduced by half, although the low activation energy and large isotope effect remain.<sup>40</sup>

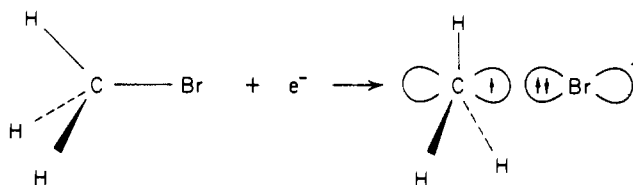
The occurrence of the abstraction reaction at low temperature is by no means limited to acetonitrile, but seems, rather, to be a general phenomenon. We have observed it in various solid matrices,<sup>41-45</sup> as have others.<sup>46</sup> One of the most striking examples of the effects caused by tunneling is seen in the abstraction by methyl radicals from methanol in methanol glass;<sup>45</sup> the abstraction rate constant becomes essentially temperature independent below about 40 K. This is attributable to the occurrence of tunneling only from the zero-point vibrational level.<sup>47</sup>

### Radical-Anion Pairs

As already mentioned, methyl bromide functions as an efficient electron scavenger in preventing the radiation-induced formation of (MeCN)<sub>2</sub><sup>-</sup> in crystal I of acetonitrile. Apart from proving the anionic nature of the paramagnetic color center, this experiment<sup>24</sup> provided the first ESR evidence for a weak interaction between the radical and anionic moieties formed by

dissociative electron attachment in a solid. This type of interaction has now been observed in many other systems,<sup>48</sup> and it clearly corresponds to an intermediate stage in the dissociation of an unstable radical anion produced by electron capture.

Instead of a simple 1:3:3:1 quartet as would be expected for the methyl radical alone, the ESR spectrum of Me<sup>-</sup>-Br<sup>-</sup> contains additional lines showing coupling to <sup>79</sup>Br and <sup>81</sup>Br nuclei.<sup>24</sup> The magnitude of the bromine couplings indicates that a small spin density (ca. 0.1) resides in the bromine 4p orbital directed along the C<sub>3</sub> symmetry axis of the radical. Also, the determination of the largest principal value of the <sup>13</sup>C hyperfine tensor<sup>29</sup> shows, just as in the case of the unbound CH<sub>3</sub> radical, that the methyl radical fragment is essentially planar. We expect, therefore, a reduction in the <sup>1</sup>H coupling to about 90% of the value from free CH<sub>3</sub>, as observed.<sup>24</sup> Thus, the geometry of the Me<sup>-</sup>-Br<sup>-</sup> species differs from that of the neutral MeBr molecule in that the methyl group has become planar and the C-Br bond has presumably lengthened. As most of the spin density is concentrated on carbon, it is more reasonable to regard the species as a radical-anion pair or adduct<sup>49</sup> than as a true radical anion. The process of electron capture is depicted schematically below.



Very similar results have been obtained for the methyl radical-iodide ion pair in the acetonitrile matrix,<sup>50</sup> the spin density transferred to the iodine 5p orbital being about 0.2.<sup>50b</sup> Since neither the shape nor the reactivity<sup>40</sup> of the methyl radical fragments in these systems is appreciably modified by the presence of the anion, it can be argued that the degree of covalent binding represented by the three-electron bond in the Me<sup>-</sup>-X<sup>-</sup> species is very small indeed. It seems probable, therefore, that the fragments are simply held together by the constrictive cage effect of the rigid crystalline solid. This is consistent with the effect of pulse annealing, which brings about the irreversible dissociation of the Me<sup>-</sup>-Br<sup>-</sup> species into free methyl radicals at 175 K.<sup>24</sup> It is also significant that very few of these adduct species have been observed in glassy matrices;<sup>48d</sup> this suggests that a disordered matrix does not generally provide a suitable cage for the entrapment of fragments adjacent to each other.

Another interesting adduct center is the methyl radical-methanesulfenate anion pair formed as a result of dissociative electron capture by dimethyl sulfoxide.<sup>51</sup>

(39) See, e.g.: Caldin, E. F. *Chem. Rev.* **1969**, *69*, 135.

(40) Sprague, E. D. *J. Phys. Chem.* **1979**, *83*, 849.

(41) Campion, A.; Williams, F. *J. Am. Chem. Soc.* **1972**, *94*, 7633.

(42) Wang, J. T.; Williams, F. *J. Am. Chem. Soc.* **1972**, *94*, 2930.

(43) Sprague, E. D. *J. Phys. Chem.* **1973**, *77*, 2066.

(44) Neiss, M. A.; Sprague, E. D.; Willard, J. E. *J. Chem. Phys.* **1975**, *63*, 1118.

(45) Hudson, R. L.; Shiotani, M.; Williams, F. *Chem. Phys. Lett.* **1977**, *48*, 193.

(46) Brunton, G.; Gray, J. A.; Griller, D.; Barclay, L. R. C.; Ingold, K. U. *J. Am. Chem. Soc.* **1978**, *100*, 4197 and references therein. Toriyama, K.; Iwasaki, M. *J. Phys. Chem.* **1978**, *82*, 2056 and references therein. Platz, M. S.; Senthilnathan, V. P.; Wright, B. B.; McCurdy, Jr., C. W. *J. Am. Chem. Soc.* **1982**, *104*, 6494.

(47) Le Roy, R. J.; Murai, H.; Williams, F. *J. Am. Chem. Soc.* **1980**, *102*, 2325 and references therein. The supplementary material available for this paper consists of tables of rate constants for hydrogen atom abstraction by methyl radicals in five different systems, including crystal I and crystal II of acetonitrile.

(48) See, e.g.: (a) Chung, Y. J.; Williams, F. *J. Phys. Chem.* **1972**, *76*, 1792. (b) Symons, M. C. R. *J. Chem. Soc., Perkin Trans. 2* **1973**, 797. Lyons, A. R.; Symons, M. C. R.; Mishra, S. P. *Nature (London)* **1974**, *249*, 341. (c) Toriyama, K.; Iwasaki, M. *J. Chem. Phys.*, **1976**, *65*, 2883. (d) Irie, M.; Shimizu, M.; Yoshida, H. *J. Phys. Chem.* **1976**, *80*, 2008; *Chem. Phys. Lett.* **1974**, *25*, 102. Brocklehurst, B.; Savadatti, M. I. *Nature (London)* **1966**, *212*, 1231.

(49) Mishra, S. P.; Symons, M. C. R. *J. Chem. Soc., Perkin Trans. 2*, **1973**, 391. Symons, M. C. R.; Smith, I. G. *Ibid.* **1979**, 1362.

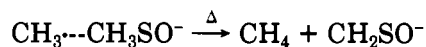
(50) (a) Fujita, Y.; Katsu, T.; Sato, M.; Takahashi, K. *J. Chem. Phys.* **1974**, *61*, 4307. (b) Symons, M. C. R.; Smith, I. G. *J. Chem. Soc., Perkin Trans. 2*, **1981**, 1180.

(51) (a) Chung, Y. J.; Nishikida, K.; Williams, F. *J. Phys. Chem.* **1974**, *78*, 1882. (b) Symons, M. C. R. *J. Chem. Soc., Perkin Trans. 2*, **1976**, 908.



In this case the hyperfine couplings to deuterium<sup>51</sup> and hydrogen<sup>52</sup> indicate that the spin density in the carbon 2p orbital of the methyl radical fragment is even smaller than that for the methyl halide adducts, the values being 0.84 for CD<sub>3</sub>---CD<sub>3</sub>SO<sup>-</sup><sup>51a</sup> and 0.82 for CH<sub>3</sub>---CH<sub>3</sub>SO<sup>-</sup>.<sup>52</sup> Although no hyperfine interaction with the nuclei in the anionic fragment could be detected, possibly owing to the very low natural abundance of the <sup>13</sup>C and <sup>33</sup>S isotopes, the center was found to have a strong optical band at 540 nm.<sup>51a</sup> This is strong additional evidence that the species is not a free methyl radical, since the electronic absorption bands of gaseous methyl radicals are located near 215 nm.<sup>53</sup>

A curious feature of the original work<sup>51a</sup> was the failure to detect the center in (CH<sub>3</sub>)<sub>2</sub>SO after  $\gamma$  irradiation at 77 K, although the species produced from (CD<sub>3</sub>)<sub>2</sub>SO was stable for several hours at this temperature. In light of our experience, it was proposed that this striking example of an "all-or-nothing" deuterium isotope effect<sup>42</sup> might be connected with the very much greater reactivity of the methyl radical fragment in H-atom abstraction at 77 K, a process which perhaps could only be arrested at much lower temperatures. This suggestion has since been substantiated by the ESR detection of the CH<sub>3</sub>---CH<sub>3</sub>SO<sup>-</sup> species below 50 K following  $\gamma$  irradiation of (CH<sub>3</sub>)<sub>2</sub>SO at 4 K.<sup>52</sup> Also, thermal decay of the center proceeds by a "geminate" H (or D) atom abstraction from the conjugate MeSO<sup>-</sup> anion. This reaction path



has been verified by studies of CD<sub>3</sub>SOCH<sub>3</sub>.<sup>54</sup> In agreement with the expectation that H-atom abstraction should take place exclusively at 77 K, the long-lived species detected at this temperature is CH<sub>3</sub>---CD<sub>3</sub>SO<sup>-</sup> and not CD<sub>3</sub>---CH<sub>3</sub>SO<sup>-</sup>.<sup>54</sup> Moreover, the decay of the

CH<sub>3</sub>---CD<sub>3</sub>SO<sup>-</sup> species exactly parallels that of the CD<sub>3</sub>---CD<sub>3</sub>SO<sup>-</sup> species at the same temperature.

### Concluding Remarks

Solid-state studies of electron attachment reactions, both nondissociative and dissociative, reveal interesting structural and chemical information about the molecular nature of these processes. In particular, ESR measurements of the spin distribution in the products allow a fairly sharp distinction to be drawn between radical anions and radical-anion pairs or adducts. Dimer radical anion formation can also take place, but the crystal structure plays a role in this process, as expected. Some radical anions undergo photolysis to give radical-anion pairs, which may then revert back to the original radical anion by a thermal reaction. The chemistry of these reversible processes is made more intricate by a competing reaction in which the radical abstracts a hydrogen atom from a neighboring molecule. However, the unraveling of this complication has also served to extend our knowledge of the role of quantum tunneling in chemical reactions.

The results of these investigations testify to the potential of solid-state techniques for the study of novel and frangible radical ions. Progress in this field shows no sign of abating, as witness the recent discovery of perfluorocycloalkane radical anions<sup>55</sup> and alkane radical cations.<sup>56</sup>

*We wish to acknowledge the contributions made by our collaborators, whose names appear in the references. This research has been supported at the University of Tennessee by the Division of Chemical Sciences, Office of Basic Energy Sciences, U.S. Department of Energy (Document No. DOE/ER/02968-119), and at the University of Cincinnati by the Research Corporation.*

(55) Shiotani, M.; Williams, F. *J. Am. Chem. Soc.* **1976**, *98*, 4006. Hasegawa, A.; Shiotani, M.; Williams, F. *Faraday Discuss. Chem. Soc.* **1977**, *63*, 157.

(56) See, e.g.: Shida, T.; Kubodera, H.; Egawa, Y. *Chem. Phys. Lett.* **1981**, *79*, 179. Wang, J. T.; Williams, F. *J. Phys. Chem.* **1980**, *84*, 3156; *Chem. Phys. Lett.* **1981**, *82*, 177. Symons, M. C. R.; Smith, I. G. *J. Chem. Res. Synop.* **1979**, 382. Iwasaki, M.; Toriyama, K.; Nunome, K. *J. Am. Chem. Soc.* **1981**, *103*, 3591; *J. Phys. Chem.* **1981**, *85*, 2149.

(52) Murai, H.; Williams, F., unpublished results.

(53) Herzberg, G. *Proc. R. Soc. London, Ser. A* **1961**, *262*, 291.

(54) Blum, A.; Wang, J. T.; Williams, F., unpublished results.